

Received November 30, 2018; reviewed; accepted January 31, 2019

Adsorption of lanthanum(III) and yttrium(III) on kaolinite: kinetics and adsorption isotherms

Fang Zhou, Jian Feng, Xiong Xie, Baihong Wu, Qi Liu, Xiaoyan Wu, Ruan Chi

Key Laboratory for Green Chemical Process of Ministry of Education, School of Chemical Engineering and Pharmacy, Wuhan Institute of Technology, Wuhan 430073, China

Corresponding author: rac513@163.com (Ruan Chi)

Abstract: Experimental investigations were carried out using kaolinite to adsorb two rare earth ions, lanthanum ion (La^{3+}) and yttrium ion (Y^{3+}), which will provide some useful information and new insights on the mineralization process and fractionation phenomenon of weathered crust elution-deposited rare earth ores. The results showed that the equilibrium adsorption capacity of Y^{3+} is greater than La^{3+} under the same experimental conditions. The adsorption of rare earth ions presents strongly temperature dependent indicating an endothermic adsorption process. The pseudo-first-order kinetic model and the pseudo-second-order kinetic model were applied to discuss the adsorption kinetics. It was found that the adsorption rate of rare earth follows the pseudo-second-order kinetic model among the adsorption temperature range. Furthermore, the adsorption process of rare earth ions on kaolinite followed the Langmuir isotherm model confirmed by the correlation of experimental equilibrium data to standard isotherm model, Langmuir and Freundlich isotherms. The activation energies for the adsorption of La^{3+} and Y^{3+} on kaolinite are 28.1903 kJ/mol and 25.4190 kJ/mol, respectively. All kaolinite before and after adsorption were characterized by XRD and SEM-EDX to understand the adsorption mechanism. The obtained results suggested that the adsorption of La^{3+} and Y^{3+} on kaolinite is an endothermic and chemisorption process.

Keywords: adsorption, kaolinite, rare earth, kinetics

1. Introduction

The Rare earth elements (REEs) include scandium (Sc), yttrium (Y) and fifteen Lanthanide elements (La, Ce, Pr, Nd, Pm, Sm, Eu, Gd, Tb, Dy, Ho, Er, Tm, Yb, Lu). However, since scandium and promethium do not co-exist with the other rare earth elements, those 15 elements are very often expressed as REEs. Based on the difference of chemical and physical property, the REEs are divided into two groups which are light and heavy rare earth elements. The light rare earth elements are La, Ce, Pr, Nd, Sm and Eu. The heavy rare earth elements are Gd, Tb, Dy, Ho, Er, Tm, Yb, Lu, Sc and Y (Chi and Tian, 2008; Zhou et al., 2017). Until recently, REEs, especially heavy REEs, have received extensive attention from mineral processing researchers due to their application and the increasing demand in high-technology industry (Lan et al., 2019). The heavy rare earth elements resources are enriched in the weathered crust elution-deposited rare earth ores in southern China, where Jiangxi and Guangdong provinces hold about 70% of the total deposits. However, the rare earth (RE) supplies are declining and uncertain, and the recycling of REEs-containing wastes is thus becoming important. All of them can decrease the contamination from rare earth discharge (Ma et al., 2019).

The weathered crust elution-deposited rare earth ores is a specific kind of ore formed by rare earth ions adsorbed on clay minerals in the form of hydrated ions or hydroxyl hydrated ions (Chi and Tian, 2008; Feng et al., 2018). The electrolyte solutions such as ammonium salt solution are usually applied to recover rare earth ions through ion-exchange reaction, which confirms that rare earth elements would migrate, fractionate and enrich on clay minerals (Nesbitt, 1979). The mineralization process of

this ore is the weathering of rare earth minerals such as granodiorite and volcanic rocks to transform into clay minerals such as kaolinite and halloysite, and then REEs in these ore changes to hydrated ions or hydroxyl hydrated ions adsorbed on clay minerals in humid and warm climate. Rare earth ions would migrate, fractionate and enrich when granodiorite rocks were weathered and transformed into clay minerals. Based on the weathering degree of ores, the weathered crust elution-deposited rare earth ores can be divided into humus layer, whole weathered layer, half weathered layer and bed rock from surface to bottom. Furthermore, the leaching of underground water and the scouring of surface water make rare earth ions in humus layer migrating and enriching downwards to the whole weathered layer. Due to the small difference of geochemical property among REEs and minerals, differentiation phenomenon will happen during the process of REEs weathered from the original rock and migration with groundwater. The heavy rare earth ions enriched at the bottom of whole weathered crust are called fractionation effect, which is due to the adsorption and desorption during the process of migration and enrichment of rare earth ions in clay minerals (Bao and Zhao, 2008; Zhang, 2016). Therefore, the adsorption and desorption of rare earth ions on clay minerals plays an important role in the mineralization process and fractionation phenomenon of weathered crust elution-deposited rare earth ores. Investigation on the adsorption of heavy rare earth ion and light rare earth ion on the clay minerals can provide some useful information on the mineralization process and fractionation phenomenon of weathered crust elution-deposited rare earth ores.

The kaolinite as the main clay minerals in weathered crust elution-deposited rare earth ores possesses fine absorption and cation exchange ability (Chi and Tian, 2008). The ion-exchange sites are located on the surface of kaolinite and it has no interlayer ion-exchange sites (Ghosh and Bhattacharyya, 2002). In this study, the lanthanum and yttrium were chosen as the representatives of light and heavy rare earth elements, respectively. Their adsorption characteristics on kaolinite were investigated to further understand the mineralization process and the fractionation phenomenon of weathered crust elution-deposited rare earth ores. The adsorption isotherm and dynamic of La^{3+} and Y^{3+} on kaolinite were discussed according to the sealing oscillation equilibrium method.

2. Materials and methods

2.1. Material and reagent

Reagents used as lanthanum nitrate, yttrium nitrate, nitric acid, ethylene diamine tetraacetic acid (EDTA), zinc oxide, ascorbic acid, sulfosalicylic acid, xylenol orange, hexamethylenetetramine, hydrochloric acid and ammonia were reagent grade. The kaolinite (CAS: 1332-58-7) was purchased from Sinopharm Chemical Reagent Co., Ltd. In the sealing oscillation equilibrium experiments, lanthanum and yttrium solutions were prepared by dissolving their nitrate in the de-ionized water.

2.2. Adsorption experiment

In the sealing oscillation equilibrium experiments, 50 mL rare earth solutions with a certain concentration were mixed with 1.0 g of Kaolinite into a conical flask to take an adsorption process placed in the constant temperature water bath vibrator (MMS-1, mettler Toledo instrument). The rare earth solutions were modified at pH 5 before adsorption, which is consistent with the weak acid environment in the mineralizing process of weathered crust elution-deposited rare earth ores (Chi and Tian 2008; Moldoveanu and Papangelakis 2016). After a filtration, rare earth concentrations before and after equilibrium were analyzed by EDTA titration method to calculate the adsorption capacity Q_e (mmol/g) and adsorption efficiency by the following equations (Zhou et al., 2017; He et al., 2016a; He et al., 2016b).

$$Q_e = \frac{(c_0 - c_e)V}{m} \quad (1)$$

$$\text{Adsorption efficiency} = \frac{(c_0 - c_e)}{c_0} \times 100\% \quad (2)$$

where, C_0 is the initial concentration of RE in solution, mmol/L. C_e is the equilibrium concentration of RE in solution, mmol/L. V is the volume of rare earth solution, mL. m is the mass of kaolinite, g. Q_e is the equilibrium adsorption capacity, mmol/g.

2.3. Characterization methods

X-ray diffraction (XRD) measurement was used to determine the crystal structure of kaolinite using a RIGAKU Rotating anode XRD system (Rigaku RU-200B) between and with a scan speed of 2 degrees per minute. The power of x-ray tube was set at 40 kV and 110 mA. Scanning electron microscope (SEM) experiments were performed using a scanning electron microscope (SEM) Vega-3 (Tescan) with an EDX detector (Oxford Instruments). The sample was placed in a vacuum chamber, coated with a thin gold (Au) metal layer. All the experiments were conducted at room temperature of 25 °C.

2.4. Adsorption kinetics

Kinetics analysis in rare earth-kaolinite system was conducted to provide quantitative and important information to try to figure out the mechanisms of adsorption processes. Moreover, the kinetics describe the solute absorption rate which in turn controls the residence time of sorbate uptake at the solid-solution interface (Jiang et al., 2018). In order to investigate the adsorption of rare earth ions on the kaolinite, pseudo-first-order kinetic model and pseudo-second-order kinetic model are applied to discuss the controlling mechanism of this adsorption process (Bai et al., 2013; Xu et al., 2013).

(a) Pseudo-first-order kinetic model

$$\frac{1}{Q_t} = \frac{k_1}{Q_e t} + \frac{1}{Q_e} \quad (3)$$

(b) Pseudo-second-order kinetic model

$$\frac{t}{Q_t} = \frac{1}{K_2 Q_e^2} + \frac{t}{Q_e} \quad (4)$$

where Q_t and Q_e are the adsorption amount of rare earth ions (mmol/g) at contact time t (h) and at equilibrium, and K_1 and K_2 are the pseudo-first-order rate constant and pseudo-second-order rate constant, respectively.

2.5. Adsorption isotherms

The fitting of adsorption isotherms to experimental data plays an important role in the adsorption process (Nandi et al., 2009). Langmuir and Freundlich isotherms are the two most commonly used adsorption isotherm equations, which was applied in this study.

(a) Langmuir isotherm

$$Q_e = \frac{Q_m K_L C_e}{1 + K_L C_e} \quad (5)$$

(b) Freundlich isotherm

$$Q_e = K_F C_e^{1/n} \quad (6)$$

where Q_e and C_e are the adsorption capacity and liquid phase concentration at equilibrium, respectively. Q_m is the maximum adsorption capacity. K_L and K_F are the Langmuir isotherm constant and Freundlich isotherm constant, respectively. n is the heterogeneity factor, indicating the degree of non-linearity between solution concentration and adsorption.

After mathematical deformation, the linear equations for Langmuir isotherm and Freundlich isotherm are shown as follows:

(a) Langmuir isotherm

$$\frac{C_e}{Q_e} = \frac{C_e}{Q_m} + \frac{1}{K_L Q_m} \quad (7)$$

(b) Freundlich isotherm

$$\log Q_e = \frac{1}{n} \cdot (\log C_e) + \log K_F \quad (8)$$

where Q_m and K_L can be obtained by the slope and intercept from the figure plotted by Equation. (7). n and K_F can be calculated by the slope and intercept from the figure plotted by Equation. (8).

3. Results and discussion

3.1. Adsorption characteristics of La^{3+} and Y^{3+} on Kaolinite

3.1.1 Effects of initial concentration of La^{3+} and Y^{3+} on the adsorption

At 298 K, the equilibrium adsorption experiments were conducted under different initial concentrations of La^{3+} and Y^{3+} and the results were shown in Fig. 1. It can be seen from Fig.1 that the variation on the adsorption curve of La^{3+} is similar to that of Y^{3+} . The equilibrium adsorption capacity of La^{3+} and Y^{3+} on kaolinite increases with increasing initial concentration until reaches equilibrium. This behaviour could be due to the fact that more adsorbing sites of kaolinite would be occupied by the lanthanum and yttrium ions with the increasing of rare earth ions contacted to kaolinite. However, the adsorption efficiencies of La^{3+} and Y^{3+} on kaolinite have the opposite variation as a function of initial concentration, indicating that the rare earth ions solutions with low concentration, when compared with their high concentration, presents a better utilization percentage of adsorbing sites of kaolinite. Moreover, the adsorption efficiencies of La^{3+} and Y^{3+} on kaolinite are lower than 25 %, confirming a small number of adsorbing sites on kaolinite surface (Ghosh and Bhattacharyya, 2002).

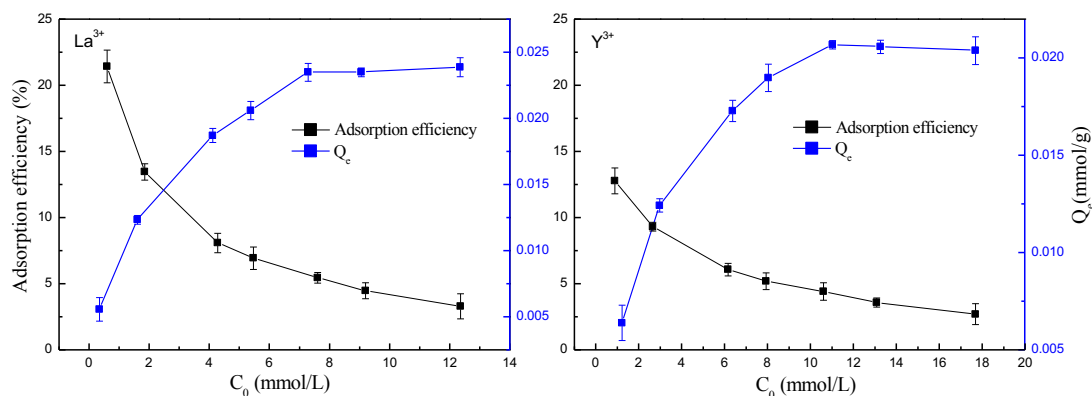


Fig. 1. Equilibrium adsorption capacity and adsorption efficiency of La^{3+} and Y^{3+} on Kaolinite as a function of initial concentration

3.1.2 Effects of temperature on the adsorption

Fig. 2 shows the effects of temperature on the equilibrium adsorption capacity of La^{3+} and Y^{3+} on kaolinite at a certain initial concentration of 1.2 g/L. Both the two equilibrium adsorption capacity of La^{3+} and Y^{3+} increases with increase in temperature, suggesting that the adsorption process of La^{3+} and Y^{3+} on kaolinite could be an endothermic behavior. Furthermore, the La^{3+} shows a lower equilibrium adsorption capacity than Y^{3+} on Kaolinite at the same temperature, which is in agreement with the literatures (Coppin et al., 2002; Moldoveanu and Papangelaki, 2016). Coppin et al. (Coppin et al., 2002) found a significant increase of the adsorption coefficient values from light rare earth to heavy rare earth. This phenomenon is due to the lower radius of Y^{3+} than La^{3+} .

3.1.3 Effects of time on the adsorption

The adsorption time is an important factor to establish a steady-state concentration. At the different adsorption temperatures, the adsorption capacity of La^{3+} and Y^{3+} on kaolinite at the same initial concentration of 1.2 g/L as a function of time were investigated shown in Fig.3. The adsorption capacity of La^{3+} and Y^{3+} on kaolinite increases with increase in the time until an equilibrium value. The equilibrium adsorption capacity of La^{3+} and Y^{3+} on kaolinite increase from 0.0155 to 0.0198

mmol/g (La^{3+}) and from 0.0174 to 0.0226 mmol/g (Y^{3+}) when the temperature increased from 283 K to 323 K, suggesting that the adsorption process of rare earth ions on kaolinite is endothermic. At relatively higher temperature, the mobility of rare earth ions in solution will be higher, hence the rare earth ions have the chance to be adsorbed in the octahedral layers of kaolinite. As a result, the equilibrium adsorption time of the system will be shorter (Al-Ghouti et al., 2005). A chemisorption may be applied to illustrate the trend that the equilibrium adsorption capacity of La^{3+} and Y^{3+} on kaolinite tends to increase with the increasing temperature, because the physisorption is usually accompanied by the experiment phenomena that the adsorption decreases with increase in temperature. The physisorption, arising from the weaker vander Waals force and dipole forces, is usually associated with low heat of adsorption (Doğan et al., 2009). Moreover, at low temperature, the desorption might be occurred. This phenomenon could be attributed to either a reversible adsorption or a back diffusion controlling mechanism (Al-Ghouti et al., 2005).

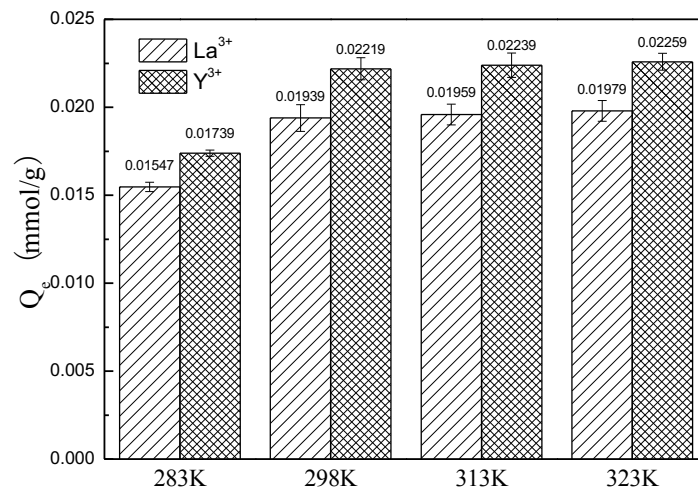


Fig. 2. Equilibrium adsorption capacity of La^{3+} and Y^{3+} on kaolinite as a function of temperature

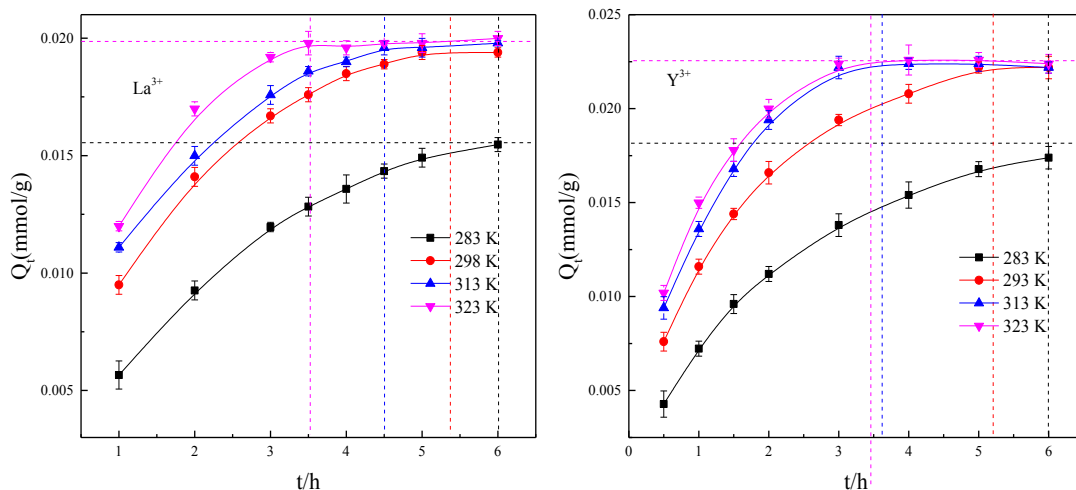


Fig. 3. Adsorption capacity of La^{3+} and Y^{3+} on kaolinite as a function of time

3.2. Kinetic analysis

In order to further investigate the adsorption characteristic of La^{3+} and Y^{3+} on the surface of kaolinite, different kinetics models are used to discuss the controlling mechanism of adsorption. The experiment data in Fig. 3 were fitted by the pseudo-first-order kinetic model and pseudo-second-order kinetic model to find the best fitted model in this study.

The pseudo-first-order kinetic model assumes that the adsorption process is considered as a reversible reaction with an equilibrium being established between two phases (Bhattacharya and Venkobachar, 1984; Wong et al., 2018). Usually, the adsorption reaction is controlled by a boundary diffusion. The fitting results for the adsorption of La^{3+} and Y^{3+} on kaolinite by pseudo-first-order kinetic model showed a poor agreement with the experimental data derived from Fig.3. Hence it is concluded that the process is non-diffusion controlled. However, regarding to the pseudo-second-order kinetic model, the better agreement was found as it is observed in Fig. 4 and Fig. 5, and Table 1 and Table 2.

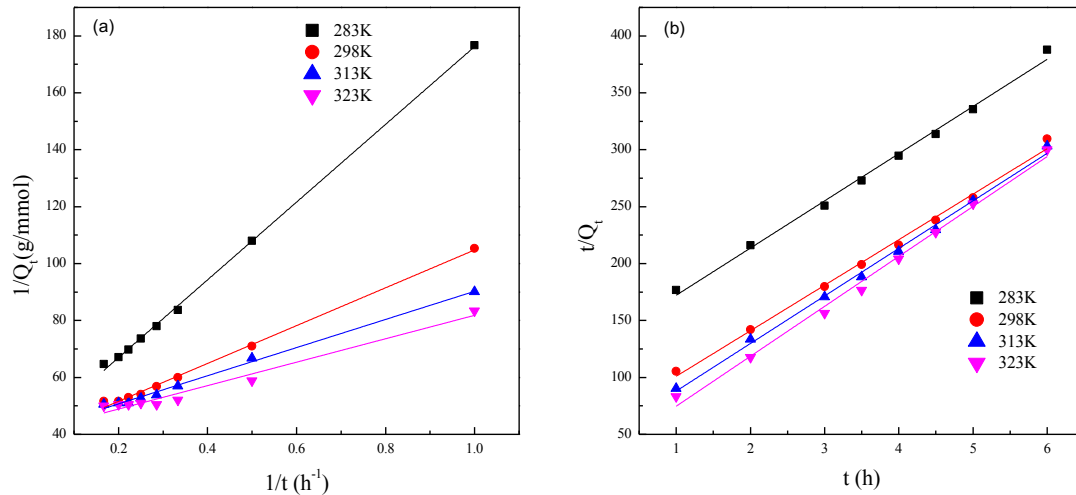


Fig. 4. Pseudo-first-order-kinetic model (a) and Pseudo-second-order-kinetic model (b) for the adsorption of La^{3+} on kaolinite

Table 1. Different kinetic model parameters for the adsorption of La^{3+} on kaolinite

Temperature (K)	Pseudo-first-order-kinetic			Pseudo-second-order-kinetic		
	$K_1(\text{h}^{-1})$	$Q_e(\text{mmol/g})$	R^2	$K_2(\text{g/mmol/h})$	$Q_e(\text{mmol/g})$	R^2
283	3.4430	0.02521	0.998	13.1489	0.02412	0.996
298	1.7345	0.02609	0.996	26.1023	0.02506	0.996
313	1.2114	0.02450	0.994	37.7213	0.02394	0.996
323	1.0127	0.02459	0.967	62.3454	0.02280	0.993

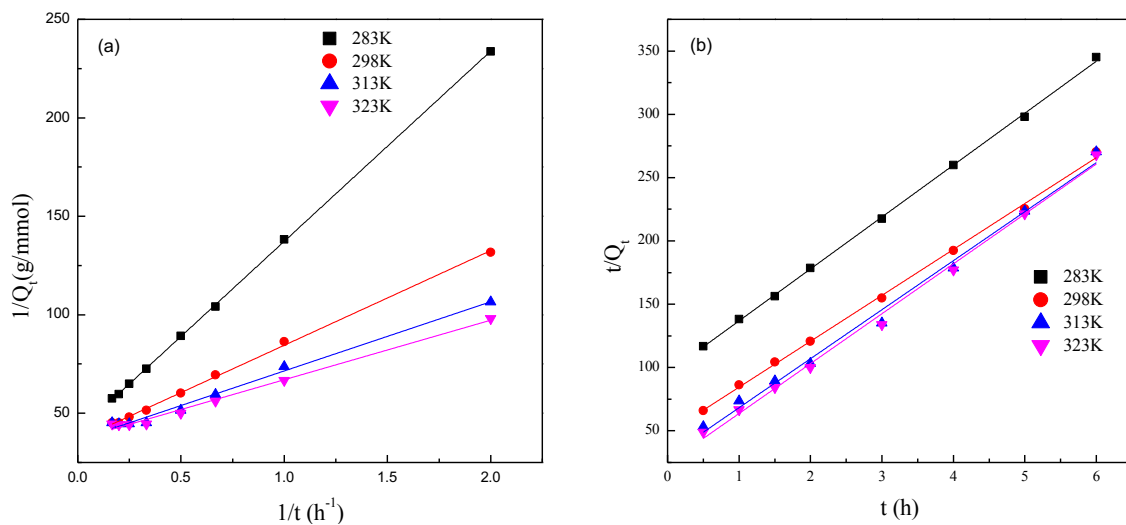


Fig. 5. Pseudo-first-order-kinetic model (a) and Pseudo-second-order-kinetic model (b) for the adsorption of Y^{3+} on kaolinite

Table 2. Different kinetic model parameters for the adsorption of Y^{3+} on kaolinite

Temperature (K)	Pseudo-first-order-kinetic			Pseudo-second-order-kinetic		
	K_1 (h ⁻¹)	Q_e (mmol/g)	R^2	K_2 (g/mmol/h)	Q_e (mmol/g)	R^2
283	2.3710	0.02455	0.998	17.5704	0.02437	0.999
298	1.3185	0.02743	0.998	27.2985	0.02757	0.998
313	0.9662	0.02750	0.990	50.8172	0.02582	0.992
323	0.8219	0.02719	0.990	64.0203	0.02537	0.995

In most cases, the adsorption with chemisorption as the rate-control follows the pseudo-second-order model (Nandi et al., 2009). Fig. 4(b) and Fig. 5(b) show that the plot of t/Q_t versus t is a straight line with slope of $1/Q_e$ and intercept of $1/(K_2Q_e^2)$. The Q_e can be calculated by the slope and then the K_2 is determined by the intercept. The K_2 , Q_e and their corresponding regression coefficient (R^2) values are listed in Table 1 for La^{3+} adsorption and in Table 2 for Y^{3+} adsorption, respectively. The values of regression coefficient for different temperatures are more than 0.992, which confirms that, the adsorption kinetics of La^{3+} and Y^{3+} on the surface of kaolinite follows the pseudo-second-order model. Furthermore, the values of Q_e calculated from Pseudo-second-order-kinetic model are closer to the equilibrium adsorption capacity shown in Fig.3, whatever for La^{3+} adsorption or Y^{3+} adsorption. Therefore, the adsorption of La^{3+} and Y^{3+} on the surface of kaolinite can be better explained by the pseudo-second-order model than the pseudo-first-order model, and this process is chemisorption controlled.

3.3. Adsorption isotherm

Adsorption properties and thermodynamics parameters are usually known as the adsorption isotherm, which can be plotted by the relationship between adsorption capacity and concentration at a certain temperature. The adsorption isotherm describes how the rare earth ions interact with kaolinite, and provides some information about the adsorption characteristics of rare earth ions on the kaolinite in this study. The isotherms adsorption of RE^{3+} -kaolinite system at 298 K are shown in Fig.6.

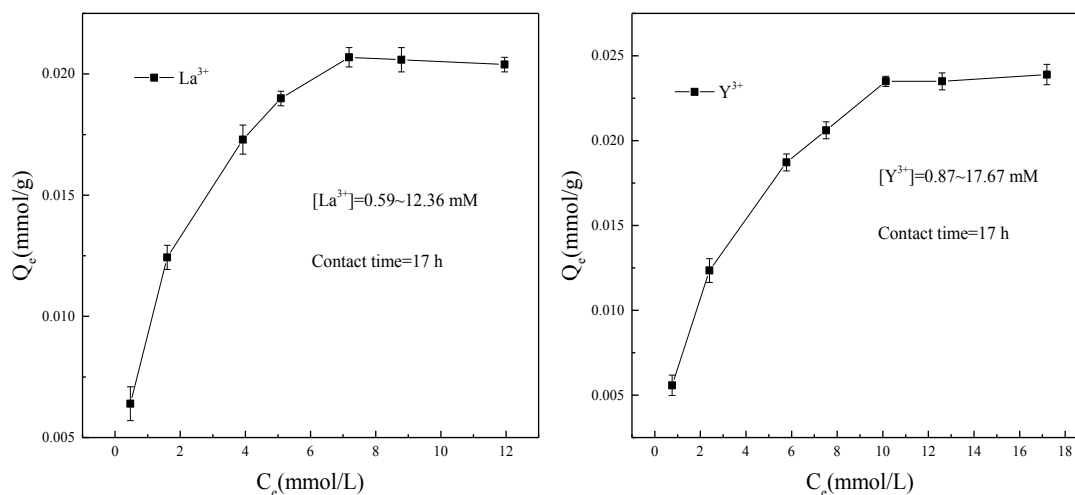


Fig. 6. Equilibrium adsorption capacity of La^{3+} and Y^{3+} on Kaolinite as a function of equilibrium concentration of REEs

Here, the adsorption data of La^{3+} and Y^{3+} from the experiments were fitted with Langmuir isotherm and Freundlich isotherm. According to Equations (7) and (8), the correlation coefficients for Langmuir and Freundlich isotherm are calculated by fitting the experimental adsorption equilibrium data in Fig. 6. The linear fit results are shown in Fig. 7 and Fig. 8, and the Langmuir and Freundlich isotherm constants calculated are shown in Table 3.

From Fig. 7 and Table 1, the correlation coefficient (R^2) of Langmuir for La^{3+} is 0.996, higher than that of Freundlich, proving Langmuir isotherm fitting well to the adsorption process of La^{3+} on

kaolinite. Moreover, the similar results can be concluded for the adsorption process of Y^{3+} on kaolinite. The Langmuir isotherm assumes that the binding sites are homogeneously distributed over the adsorbent surface, which describes the formation of a monolayer adsorbate on the adsorbent surface. It is a single molecular layer adsorption and no interaction between adsorbed molecules. The Freundlich isotherm is applied to the adsorption on heterogeneous surfaces. The value of $1/n$ below one indicates a normal adsorption (Nandi et al., 2009). The better fit by Langmuir isotherm indicates that the rare earth ions reacts with kaolinite in aqueous. Here, it is the chemisorption rather than physisorption. Monolayer coverage of rare earth ions, La^{3+} and Y^{3+} , is taking place over the kaolinite surface.

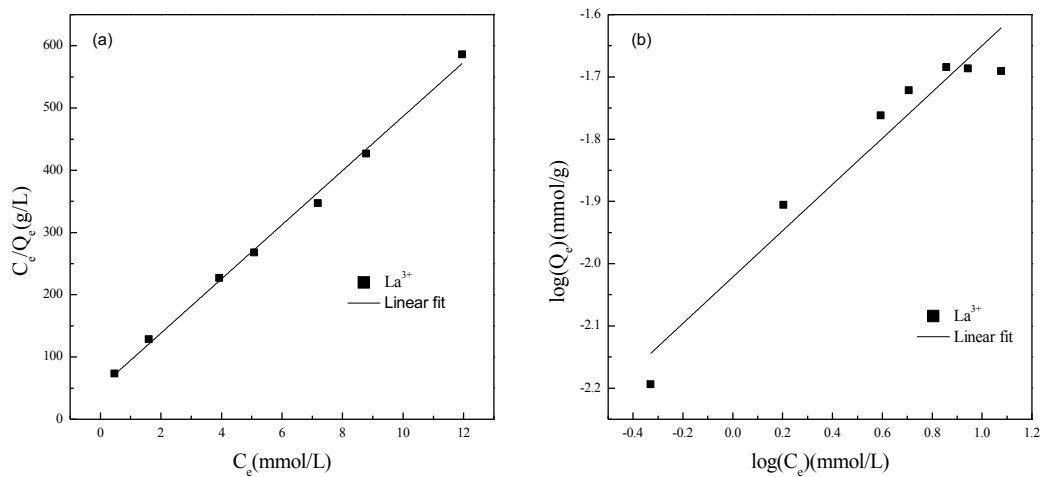


Fig. 7. Langmuir (a) and Freundlich (b) adsorption isotherm of La^{3+} on kaolinite

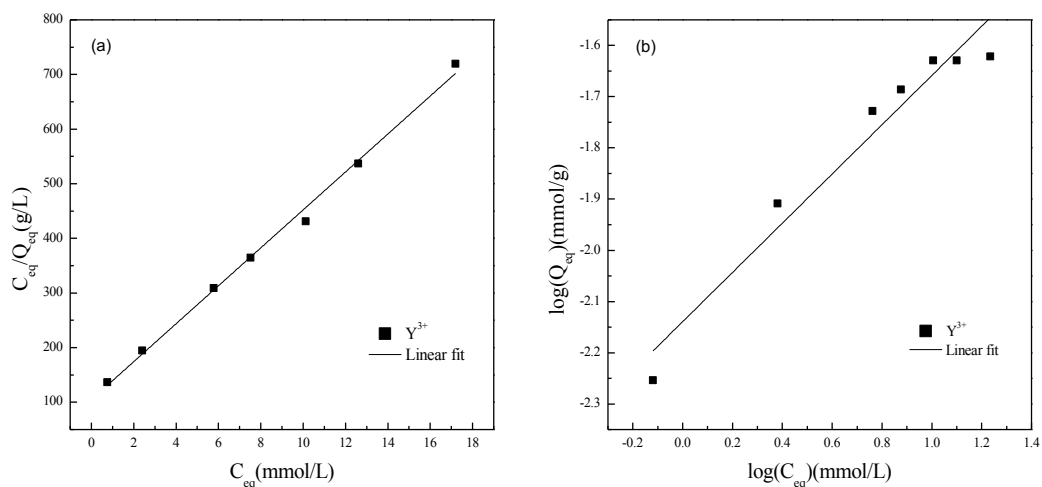


Fig. 8. Langmuir (a) and Freundlich (b) adsorption isotherm of Y^{3+} on kaolinite

Table 3. Langmuir and Freundlich isotherm constants for the adsorption of La^{3+} and Y^{3+} on kaolinite

Metal ion	Langmuir constants			Freundlich constants		
	$Q_{max}(\text{mmol/g})$	$K_L(\text{L/mmol})$	R^2	$1/n$	$K_F(\text{L/mmol})$	R^2
La^{3+}	0.02297	0.0882	0.996	0.3721	0.0095	0.929
Y^{3+}	0.02878	0.3316	0.995	0.4806	0.0072	0.942

3.4. Adsorption activation energy of La^{3+} and Y^{3+} on Kaolinite

From the rate constant K_2 in Table 1 and 2, the activation energies (E) for the adsorption of La^{3+} and Y^{3+} on kaolinite were determined using the Arrhenius equation as follows:

$$\ln k = \ln A - \frac{E}{RT} \quad (9)$$

where E , R and A are the Arrhenius activation energy, the gas constant and the Arrhenius factor, respectively.

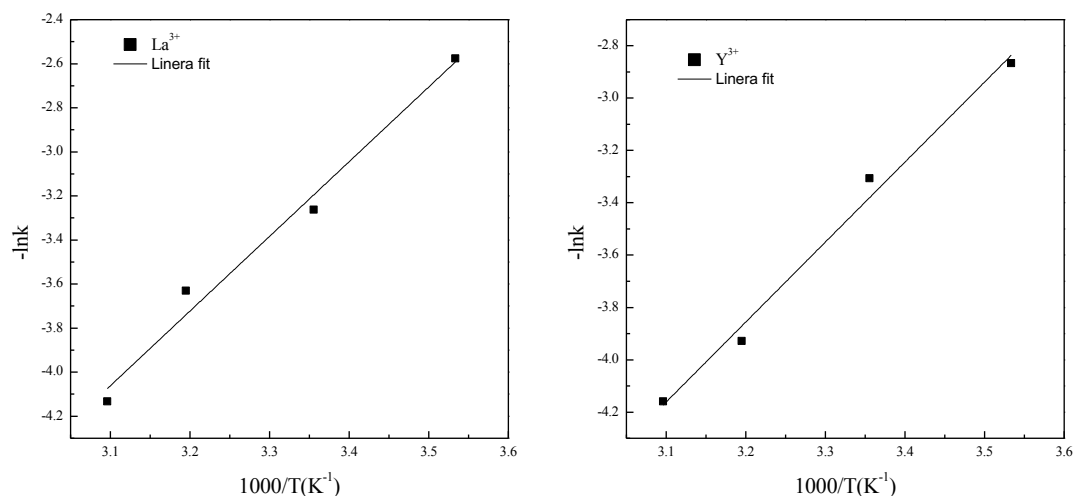


Fig. 9. Arrhenius plot for adsorption of La^{3+} and Y^{3+} on kaolinite

The Arrhenius plot of $-\ln k$ against of $1000/T$ for the adsorption of rare earth ions on kaolinite shown in Fig. 9. Based on the Equation. (9) and the Fig.9, the activation energy values for La^{3+} and Y^{3+} were calculated as 28.1903 kJ/mol and 25.4190 kJ/mol, respectively. The value of activation energy may give an idea about the type of this adsorption process, physical or chemical. Since the forces involved in physical adsorption are usually weak, an adsorption equilibrium can be attained quickly, and a small energy, no more than 4.2 kJ/mol, is required for physical adsorption (Unuabonah et al., 2007). In chemical adsorption, the force is much stronger than in physical adsorption, because the activation energy is connected with the heat of chemical reaction. Thus, the activation energy, 28.1903 kJ/mol and 25.4190 kJ/mol, are of the same magnitude as the heat of chemical reactions, confirming that the adsorption of La^{3+} and Y^{3+} on kaolinite is a chemical adsorption.

3.5. Kaolinite characterization before and after adsorption

3.5.1 XRD analysis

The XRD patterns of kaolinite before and after adsorption are presented in Fig.10. It shows that no significant change on kaolinite after adsorption could be observed. But the intensities of kaolinite main reflections presented a little decrease and a minor mobility of main reflections was observed, which may be due to the adsorption La^{3+} and Y^{3+} on kaolinite, and the small adsorption capacity leads to indistinct change in XRD patterns.

3.5.2 SEM-EDX study

The SEM and qualitative composition analysis (EDX) of kaolinite before and after adsorption are shown in Fig.11. The morphology characteristics of kaolinite can be observed, which shows a graininess. The voids and pores make the La^{3+} and Y^{3+} easy to access and adsorb. When the solution containing La^{3+} and Y^{3+} diffuses into the interior of kaolinite, La^{3+} and Y^{3+} can be easily captured by the active site of kaolinite. Moreover, the morphology of kaolinite by the SEM images are more rough and porous after adsorption, which may be due to the adsorption of La^{3+} and Y^{3+} . The adsorption capacity of clay minerals is usually affected by their surface morphology (Alshameri et al., 2018). Herein, this study has also confirmed the important role of surface morphology in the adsorption process. The EDX spectra of kaolinite before and after adsorption revealed the existence of O, Al, Si, K, Ca, Ti and Fe. After adsorption, the cations of K^+ and Ca^{2+} in kaolinite present a tiny decrease from

0.34 wt% and 0.33 wt% to 0.22 wt% and 0.25 wt%, respectively. These results suggest a possibility of cation exchange between rare earth ions and exchangeable cations in kaolinite.

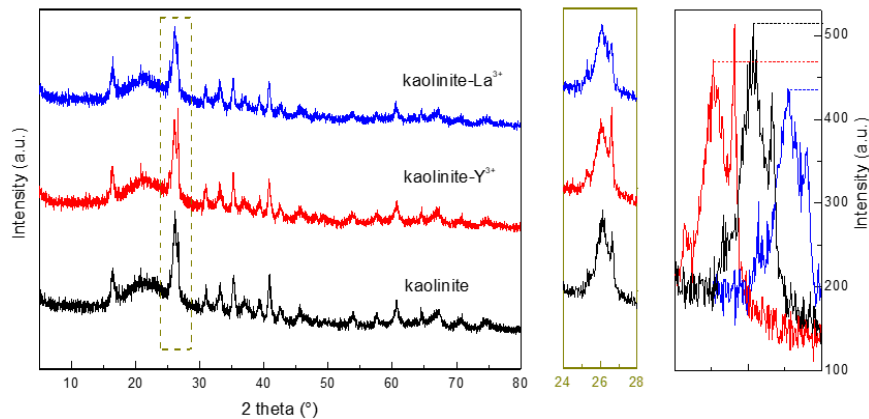


Fig. 10 XRD patterns of Kaolinite before and after adsorption

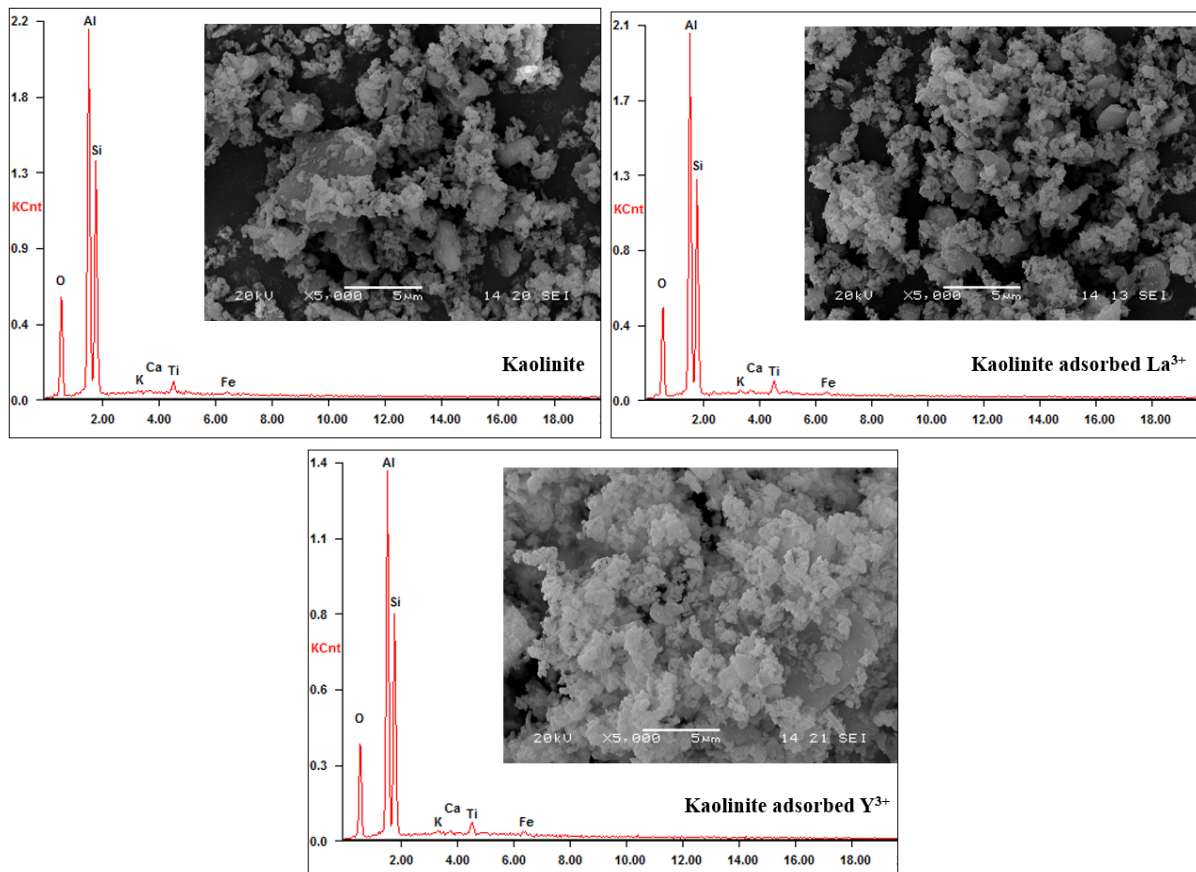


Fig.11 SEM and EDX analysis of kaolinite before and after adsorption

4. Conclusions

Results of this study provide a discussion of adsorption characteristics of La^{3+} and Y^{3+} on kaolinite. The adsorption capacity of La^{3+} and Y^{3+} on kaolinite is dependent on the initial rare earth concentration, temperature and adsorption time. The equilibrium adsorption capacity of rare earth ions on kaolinite is enhanced by their initial concentration, but the adsorption efficiency is weakened. The equilibrium adsorption capacity increases from 0.0155 to 0.0198 mmol/g for La^{3+} and from 0.0174 to 0.0226 mmol/g for Y^{3+} with increase in temperature. The endothermic process is confirmed by the fact that the equilibrium adsorption capacity of La^{3+} and Y^{3+} on kaolinite increase with increase in the

solution temperature. The adsorption kinetics of La^{3+} and Y^{3+} on kaolinite were found to follow the pseudo-second-order kinetic model, suggesting that the adsorption property of kaolinite to La^{3+} and Y^{3+} is associated to the adsorption active site on kaolinite surface. Moreover, the Langmuir isotherm model shows a good fit on the adsorption process of rare earth ions on kaolinite. The activation energy for the adsorption of La^{3+} and Y^{3+} on kaolinite are 28.1903 kJ/mol and 25.4190 kJ/mol, respectively. Thus, a chemisorption rather than physisorption can be expected, which is further confirmed by XRD and SEM/EDX characterization. All the results on the adsorption behaviour of rare earth ions on kaolinite will help understand the mineralization process and fractionation phenomenon of weathered crust elution-deposited rare earth ores.

Acknowledgments

Financial supports for this work from National Natural Science Foundation of China (51874212, 51734001 and U1802252) (China) are greatly appreciated.

References

- AL-GHOUTI, M., M. KHRAISHEH, A. M., AHMAD, M. N. M., ALLEN, S., 2005. *Thermodynamic behaviour and the effect of temperature on the removal of dyes from aqueous solution using modified diatomite: a kinetic study*. J. Colloid Interf. Sci. 287(1), 6-13.
- ALSHAMERI, A., HE, H., ZHU, J., XI, Y., ZHU, R., MA, L., TAO, Q., 2018. *Adsorption of ammonium by different natural clay minerals: Characterization, kinetics and adsorption isotherms*. Appl. Clay Sci. 159, 83-93.
- BHATTACHARYA, A. K., VENKOBACHAR, C., 1984. *Removal of cadmium (II) by low cost adsorbents*. J. Environ Eng. 110(1), 110-122.
- BAO, Z. W., ZHAO, Z. H., 2008. *Geochemistry of mineralization with exchangeable REY in the weathering crusts of granitic rocks in South China*. Ore Geol. Rev. 33(3-4), 519-535.
- BAI, F., YE, G., CHEN, G., WEI, J., WANG, J., CHEN, J., 2013. *Highly selective recovery of palladium by a new silica-based adsorbent functionalized with macrocyclic ligand*. Sep. Purif. Technol., 106, 38-46.
- COPPIN, F., BERGER, G., BAUER, A., CASTET, S., LOUBET, M., 2002. *Sorption of Lanthanides on Smectite and Kaolinite*. Chem. Geol. 182, 57-68.
- CHI, R. A., TIAN, J., 2008. *Weathered Crust Elution - deposited Rare Earth Ores*. New York: Nova Science Pub Inc., New York, USA.
- DOGAN, M., KARAOGLU, M. H., ALKAN, M., 2009. *Adsorption kinetics of maxilon yellow 4GL and maxilon red GRL dyes on kaolinite*. J. Hazard Mater. 165(1-3), 1142-1151.
- FENG, J., ZHOU, F., CHI, R. A., LIU, X., XU, Y. L., LIU, Q., 2018. *Effect of a novel compound on leaching process of weathered crust elution-deposited rare earth ore*. Miner. Eng. 129, 63-70.
- GHOSH, D., BHATTACHARYYA, K. G., 2002. *Adsorption of methylene blue on kaolinite*. Appl. Clay Sci. 20(6), 295-300.
- HE, Z. Y., ZHANG, Z. Y., YU, J. X., XU, Z. G., CHI, R. A., 2016a. *Process optimization of rare earth and aluminum leaching from weathered crust elution-deposited rare earth ore with compound ammonium salts*. J. Rare Earth, 34(4), 413-419.
- HE, Z. Y., ZHANG, Z. Y., YU, J. X., ZHOU, F., XU, Y. L., XU, Z. G., CHEN, Z., CHI, R. A., 2016b. *Kinetics of column leaching of rare earth and aluminum from weathered crust elution-deposited rare earth ore with ammonium salt solutions*. Hydrometallurgy, 163, 33-39.
- JANG, H. M., YOO, S., CHOI, Y. K., PARK, S., KAN, E., 2018. *Adsorption isotherm, kinetic modeling and mechanism of tetracycline on Pinus taeda-derived activated biochar*. Bioresource technol. 259, 24-31.
- LAN, X., GAO, J., LI, Y., GUO, Z., 2019. *A Green Method of Respectively Recovering Rare Earths (Ce, La, Pr, Nd) from Rare-Earth Tailings under Super-Gravity*. J. Hazard Mater. 367, 473-481.
- MOLDOVEANU, G. A., PAPANGELAKI, V. G., 2016. *An overview of rare-earth recovery by ion-exchange leaching from ion-adsorption clays of various origins*. Mineral Mag. 80(1), 63-76.
- MA, L., DANG, D. H., WANG, W., EVANS, R. D., WANG, W. X., 2019. *Rare earth elements in the Pearl River Delta of China: Potential impacts of the REE industry on water, suspended particles and oysters*. Environ. Pollut. 244, 190-201.
- NESBITT, H. W., 1979. *Mobility and fractionation of rare earth elements during weathering of a granodiorite*. Nature. 279, 206-210.

- NANDI, B. K., GOSWAMI, A., PURKAIT, M. K., 2009. *Adsorption characteristics of brilliant green dye on kaolin*. J. Hazard Mater. 161(1), 387-395.
- UNUABONAH, E. I., ADEBOWALE, K. O., OLU-OWOLABI, B. I., 2007. *Kinetic and thermodynamic studies of the adsorption of lead (II) ions onto phosphate-modified kaolinite clay*. J. Hazard Mater. 144(1-2), 386-395.
- WONG, S., YAC'COB, N. A. N., NGADI, N., HASSAN, O., INUWA, I. M., 2018. *From pollutant to solution of wastewater pollution: Synthesis of activated carbon from textile sludge for dye adsorption*. Chinese J. Chem. Eng. 26(4), 870-878.
- XU, Y., KIM, S. Y., ITO, T., TADA, T., HITOMI, K., ISHII, K., 2013. *Adsorption properties and behavior of the platinum group metals onto a silica-based (Crea+ TOA)/SiO₂-P adsorbent from simulated high level liquid waste of PUREX reprocessing*. J. Radioanal. Nucl. Ch., 297(1), 41-48.
- ZHOU, F., FENG, J., WANG, Z. Q., XU, Y. L., ZHANG, Z. Y., CHI, R. A., 2017. *One step purification of impurities in the leachate of weathered crust elution-deposited rare earth ores*. Physicochem. Probl. Mi. 53(2), 1188-1199.
- ZHANG, Z. Y., HE, Z. Y., YU, J. X., XU, Z. G., CHI, R. A., 2016. *Novel solution injection technology for in-situ leaching of weathered crust elution-deposited rare earth ores*. Hydrometallurgy, 164, 248-256.